Molecular Cancer Research

Genome-Wide Analysis Identifies MEN1 and MAX Mutations and a Neuroendocrine-Like Molecular Heterogeneity in Quadruple WT GIST

Maria A. Pantaleo[1,2], Milena Urbini[2], Valentina Indio[2], Gloria Ravegnini[3], Margherita Nannini[1], Matilde De Luca[2], Giuseppe Tarantino[2], Sabrina Angelini[3], Alessandro Gronchi[4], Bruno Vincenzi[5], Giovanni Grignani[6], Chiara Colombo[4], Elena Fumagalli[4], Lidia Gatto[1], Maristella Saponara[1], Manuela Ianni[2], Paola Paterini[7], Donatella Santini[8], M. Giulia Pirini[8], Claudio Ceccarelli[1], Annalisa Altimari[8], Elisa Gruppioni[8], Salvatore L. Renne[4], Paola Collini[4], Silvia Stacchiotti[4], Giovanni Brandi[1], Paolo G. Casali[4], Antonio D. Pinna[9], Annalisa Astolfi[2], and Guido Biasco[1,2]

Abstract

Quadruple wild-type (WT) gastrointestinal stromal tumor (GIST) is a genomic subgroup lacking KIT/PDGFRA/RAS pathway mutations, with an intact succinate dehydrogenase (SDH) complex. The aim of this work is to perform a wide comprehensive genomic study on quadruple WT GIST to improve the characterization of these patients. We selected 14 clinical cases of quadruple WT GIST, of which nine cases showed sufficient DNA quality for whole exome sequencing (WES). NF1 alterations were identified directly by WES. Gene expression from whole transcriptome sequencing (WTS) and miRNA profiling were performed using fresh-frozen, quadruple WT GIST tissue specimens and compared with SDH and KIT/PDGFRA-mutant GIST. WES identified an average of 18 somatic mutations per sample. The most relevant somatic oncogenic mutations identified were in TP53, MEN1, MAX, FGF1R, CHD4, and CTDNN2. No somatic alterations in NF1 were identified in the analyzed cohort. A total of 247 mRNA transcripts and 66 miRNAs were differentially expressed specifically in quadruple WT GIST. Overexpression of specific molecular markers (COL22A1 and CALCRL) and genes involved in neural and neuroendocrine lineage (ASCL1, Family B GPCRs) were detected and further supported by predicted miRNA target analysis. Quadruple WT GIST show a specific genetic signature that deviates significantly from that of KIT/PDGFRA-mutant and SDH-mutant GIST. Mutations in MEN1 and MAX genes, a neural-committed phenotype and upregulation of the master neuroendocrine regulator ASCL1, support a genetic similarity with neuroendocrine tumors, with whom they also share the great variability in oncogenic driver genes.

Implications: This study provides novel insights into the biology of quadruple WT GIST that potentially resembles neuroendocrine tumors and should promote the development of specific therapeutic approaches. *Mol Cancer Res; 15(5); 553–62.* *©2017 AACR.*

Introduction

Approximately 10% to 15% of adult cases of gastrointestinal stromal tumors (GIST) do not harbor mutations in KIT or platelet-derived growth factor receptor alpha (PDGFRA) receptors and are often referred to as KIT/PDGFRA wild-type (WT) GIST (1).

Between 20% and 40% of KIT/PDGFRA WT GIST show loss of function of the succinate dehydrogenase complex (SDH), designated as *SDH-deficient* GIST or SDHB-negative GIST based on the loss of subunit B (SDHB) protein expression (2–4). The most frequent identifiable molecular events found in SDH-deficient GIST are germline and/or somatic loss-of-function mutations in any of the four SDH subunits (A, B, C, or D), with a prevalence of the subunit A involvement (4–7). Additionally, a genome-wide DNA hypermethylation or miRNA specific profile has been associated with SDH-deficient GIST (8–12). SDH-deficient GIST have distinctive clinicopathologic features, including a predilection for young women, gastric localization, mixed epithelioid and spindle cell morphology,

[1]Department of Specialized, Experimental and Diagnostic Medicine, Sant'Orsola-Malpighi Hospital, University of Bologna, Bologna, Italy. [2]"Giorgio Prodi" Cancer Research Center, University of Bologna, Bologna, Italy. [3]Department of Pharmacy and Biotechnology, FaBit; University of Bologna, Bologna Italy. [4]Fondazione IRCCS Istituto Nazionale dei Tumori, Milan, Italy. [5]Medical Oncology, University Campus Bio-Medico, Rome, Italy. [6]Sarcoma Unit, Candiolo Cancer Institute–FPO, Torino, Italy. [7]Department of Medical and Surgical Sciences, University of Bologna, Italy. [8]Pathology Service, Addarii Institute of Oncology, Bologna, Italy. [9]General Surgery and Transplant Unit, Department of Medical and Surgical Sciences, Sant'Orsola-Malpighi Hospital, University of Bologna, Bologna, Italy.

Note: Supplementary data for this article are available at Molecular Cancer Research Online (http://mcr.aacrjournals.org/).

A. Astolfi and G. Biasco contributed equally to this article.

Corresponding Author: Maria A. Pantaleo, Department of Specialized, Experimental and Diagnostic Medicine, Sant'Orsola-Malpighi Hospital, University of Bologna, Via Massarenti 9, 40138 Bologna, Italy. Phone: 39-051-2144078; Fax: 39-051-6364037; E-mail: maria.pantaleo@unibo.it

doi: 10.1158/1541-7786.MCR-16-0376

diffuse KIT and ANO1 (DOG1) IHC positivity, frequent lymph node metastases, and an indolent disease, even when metastases are present (2, 3, 13). Moreover, SDHB IHC-negative GIST are characterized by overexpression of the insulin growth factor 1 receptor (IGF1R; refs. 14, 15). Many of these GIST arise in the context of the Carney–Stratakis syndrome (the dyad of GIST and paraganglioma), and are characterized by germline SDHB, SDHC, or SDHD inactivating mutations (16). They also occur in the context of the Carney Triad (gastric GIST, paraganglioma, and pulmonary chondroma) and may be characterized by SDHC hypermethylation (17, 18).

Amongst the KIT/PDGFRA WT GIST, the remaining cases include a subgroup harboring mutations in BRAF/RAS or NF1 and are referred to as RAS pathway (RAS-P) mutant GIST (approximately 15% of cases; refs. 19, 20); lastly, we distinguish a subgroup lacking mutations in the KIT/PDGFRA or RAS pathways, and retaining an intact SDH complex referred to as *quadruple WT* GIST (approximately 50% of KIT/PDGFRA WT GIST and 5% of all GIST; ref. 21). A massively parallel sequencing and gene expression study on two cases of *quadruple WT* GIST showed a distinct transcriptome profile profoundly different from SDHA-mutated GIST and KIT/PDGFRA mutated GIST, suggesting a different molecular background (22). Moreover, in recent reports, NF1 mutations, an MYC-associated factor X (MAX) mutation, and the ETV6–NTRK3 fusion have been described as novel molecular events in *quadruple* WT GIST (23–26).

The aim of this work is to improve the diagnostic process of *quadruple* WT GIST through a wide comprehensive molecular characterization of this subset of patients, essential for the identification of the driver molecular abnormalities as potential markers and targets of new treatments.

Materials and Methods

Patients and tumor samples

All the patients included in the study were *quadruple* WT GIST, being negative for mutations in KIT, PDGFRA, SDH, and RAS-P genes. All the cases were reported as being sporadic, lacking any personal or familiar history of a cancer prone disease. This study was approved by the local institutional ethical committee of Azienda Ospedaliero-Universitaria Policlinico S.Orsola-Malpighi (number 113/2008/U/Tess). GIST diagnosis was based on histologic evaluation and on immunohistochemistry of CD117 and DOG1 reviewed by expert pathologists.

Selection of *quadruple* WT GIST started from 30 KIT/PDGFRA WT GIST from adult patients without any personal or familial history of cancer. BRAF and KRAS mutational status was assessed by Sanger sequencing, while SDH deficiency was assessed by IHC for SDHB. We excluded 15 samples that showed SDH deficiency and one that carried the common BRAF V600E mutation, therefore identifying 14 cases that resulted BRAF–KRAS/KIT/PDGFRA WT and SDH intact. Only nine samples (4 fresh frozen and 5 FFPE samples) had sufficient DNA quality and yield for whole exome sequencing (WES), while whole transcriptome sequencing (WTS) and miRNA profiling were performed on 4 of the *quadruple* WT cases for which fresh-frozen tissue was available. Fresh tissue specimens were collected during surgical operation, snap-frozen in liquid nitrogen and stored at −80°C until analysis. NF1 alterations were identified directly by WES and mapping of the variants on the HGMD database (www.hgmd.cf.ac.uk). Moreover, WES analysis of matched peripheral blood (PB) as normal counterpart was performed to exclude germinal mutations. Patient's characteristics are listed in Table 1.

In order to further characterize *quadruple* WT GIST, we compared their molecular analyses and profiling to other GIST subsets; to this end, SDH-deficient GIST and KIT/PDGFRA-mutant GIST were analyzed. In particular, for gene expression profiles, 4 *quadruple* WT were analyzed in comparison to 14 mutated GIST (2 SDH, 5 PDGFRA, and 7 KIT), while for miRNA profiling 4 *quadruple* WT were compared with 4 SDH-deficient and 4 KIT/PDGFRA-mutant GIST.

Whole transcriptome paired-end RNA sequencing (WTS) and WES

For WTS analysis, total RNA was extracted from tumor specimens with the RNeasy Mini Kit (Qiagen), then cDNA libraries were synthesized from 250 ng of total RNA with TruSeq RNA Sample Prep Kit v2 (Illumina) according to the manufacturer's recommendations. Briefly, poly(A)-RNA molecules were purified using oligo-dT magnetic beads, then mRNA was fragmented and randomly primed for reverse transcription, followed by second-strand synthesis to create double-stranded cDNA fragments. The generated cDNA fragments went through a terminal-end repair process and ligation using paired-end sequencing adapters, then amplified to create the final cDNA library.

For WES analysis, genomic DNA was extracted from fresh-frozen tumor specimens and from matched PB with QiAmp DNA mini kit (Qiagen) or with QiAmp DNA micro kit (Qiagen) if the tumor sample was from FFPE block. Libraries were synthesized with Nextera Rapid Capture Exome Kit (Illumina) following the manufacturer's recommendations. Briefly genomic DNA (50 ng for fresh frozen and 100 ng for FFPE samples) was tagged and fragmented by the Nextera transposome technique to an average library size of 290 bp. DNA libraries were then denatured to single-stranded DNA and hybridized to biotin-labeled 80-mer

Table 1. Patient characteristics

Patient ID	Sex	Age	Site	Size (cm)	Mitotic count	Risk classification	Lymph node metastasis	Distant metastasis	Tumor tissue type	Molecular analysis
GIST127	F	63	Ileum	5–10	6–10/50HPF	High	No	Yes	Fresh tissue	WES+WTS
GIST133	M	57	Duodenum	1.6	<5/50HPF	Very low	No	No	Fresh tissue	WES+WTS
GIST400	M	69	Duodenum	NA	NA	NA	No	No	Fresh tissue	WES+WTS
GIST401	F	45	Duodenum	NA	NA	NA	No	No	Fresh tissue	WES+WTS
GIST409	M	45	Jejunum	NA	NA	NA	No	No	FFPE	WES
GIST279	F	41	Colon	8	80/50HPF	High	No	Yes	FFPE	WES
GIST257	F	73	Ileum	12	100/50HPF	High	No	No	FFPE	WES
GIST268	M	50	Ileum	8,5	2/50HPF	Intermediate	No	No	FFPE	WES
GIST320	M	73	Ileum	13	<5/50HPF	High	No	No	FFPE	WES

probes designed to enrich 214,126 targeted exonic regions, then eluted from magnetic beads and amplified.

WTS and WES libraries were quality checked and sized with Agilent DNA 7500 chips on the Bioanalyzer 2100 (Agilent Technologies), then quantified using a fluorometric assay (Quant-iT PicoGreen Assay, Life Technologies). Paired-end libraries (12 pmol/L) were amplified and ligated to the flowcell by bridge PCR, and sequenced at 2×80 bp read length for WTS and 2×100 bp for WES, using Illumina Sequencing by synthesis (SBS) technology.

miRNA profiling

miRNA profiling was performed using TaqMan Low Density Arrays (Applied Biosystems), pools A and B, which allow to analyze 754 miRNA. Total RNA was isolated from tumor samples and retrotranscribed using the TaqMan MicroRNA Reverse Transcription Kit (Applied Biosystems) and MegaPlex RT primers (Applied Biosystems) pools A and B. cDNAs were preamplified using TaqMan PreAmp Master Mix and PreAmp primers (pools A and B; Applied Biosystems). The array cards were loaded with the preamplified sample and run on the 7900HT Fast Real-Time PCR System (Applied Biosystems).

Bioinformatic analysis

After demultiplexing and FASTQ generation (both steps performed with bcltofastq function developed by Illumina), the paired-end reads were trimmed using AdapterRemoval (https://github.com/MikkelSchubert/adapterremoval) with the aim of removing stretches of low quality bases (<Q10) and Truseq/Nextera rapid capture adapters present in the sequences. The paired-end reads were then aligned on human reference genome HG19 (www.http://genome.ucsc.edu) and analyzed with two different pipelines for WTS and WES data. Sequences coming from RNA-seq were mapped with the algorithms TopHat/BowTie (27) and the PCR and optical duplicates were removed with the function *rmdup* of Samtools (http://samtools.sourceforge.net). Gene expression profiling analysis was carried on first by adopting the function htseq-count (Python package Htseq: http://www.huber.embl.de/HTSeq/doc/overview.html) to quantify the number of reads mapped on genes included in the Ensembl release 72 annotation features (http://www.ensembl.org). Second, the evaluation of differential expressed genes was performed with the R-Bioconductor package *edgeR* and *limma* (https://bioconductor.org/) respectively to normalize and to compute the statistical analysis of differential gene expression between quadruple WT and mutated GIST.

Principal component analysis of gene expression profiling was performed with the function *prcomp* from *stats* R packages (https://www.r-project.org), while Multiple Experiment Viewer (http://mev.tm4.org) was adopted to the supervised hierarchical clustering using the Manhattan distance and the average linkage method. In order to identify the pathways overrepresented, we performed a gene set enrichment analysis with the WEB-based GEne SeT AnaLysis Toolkit (http://www.webgestalt.org) using as a priori gene sets the KEGG pathways database. DeFuse (http://compbio.bccrc.ca/software/defuse/), ChimeraScan (https://code.google.com/archive/p/chimerascan/), Tophatfusion (https://ccb.jhu.edu/software/tophat/fusion_index.shtml), and FusionMap (http://www.arrayserver.com/wiki/index.php?title=FusionMap) methods were used to detect chimeric transcripts from RNA-seq data.

miRNA data were analyzed with SDS Relative Quantification Software version 2.4. (Applied Biosystems); and miRNA with Ct values $\geq$35 were considered as not expressed and excluded from further analysis. Normalization was carried out by subtracting the mean Ct from individual Ct values. R-Bioconductor package *limma* was adopted to evaluate the differential expression profile between the quadruple WT and mutated GIST. For each of the significant differentially deregulated miRNA, the set of target genes were identified with the aims to reach the miRNA/mRNA network. The validated targets were obtained from the miRTarBase database (http://microrna.sanger.ac.uk/) that contains miRNA–target interactions (MTI) with experimental support. The predicted targets were retrieved from TargetScan (http://www.targetscan.org), DianaLab (http://diana.imis.athena-innovation.gr), miRAnda (http://www.microrna.org), mirDB (http://mirdb.org), and miRTarBase.

Using this information, miRNA array and mRNA from RNA-seq were analyzed to highlight pairs of mRNA/miRNA with opposite trends (UP vs. DOWN and vice versa).

Data from WES were mapped with Burrows-Wheeler Aligner with the default setting (28); the PCR and optical duplicates were removed as previously described for the RNA-seq, Genome Analysis Toolkit (https://software.broadinstitute.org/gatk) were used to locally realign, recalibrate, and call the Ins/del variants, while point mutations were identified with the algorithm Mutect (https://www.broadinstitute.org/cancer/cga/mutect). Single-nucleotide variants (SNV) and ins/del were annotated with a gene and protein alteration using Annovar (http://annovar.openbioinformatics.org); nonsynonymous and nonsense SNV, frameshift/non-frameshift Indels, and splice-site mutations were selected with a threshold read depth $\geq 15\times$ and a variant allele frequency $\geq$0.2. All the variants were filtered in order to select novel or rare events (frequency in the population <1%) basing on database of human variability dbSNP (http://www.ncbi.nlm.nih.gov/SNP), 1000 Genomes (http://www.1000genomes.org), ExAC (http://exac.broadinstitute.org), and EVS (http://evs.gs.washington.edu/EVS). In-depth evaluation of high confidence somatic variants was performed by verifying the presence of alternate allele on the normal counterpart and manually visualizing each variation with the *tview* function of Samtools. Potential candidate drivers were highlighted considering the Catalog of Somatic Mutations in Cancer (http://cancer.sanger.ac.uk/cosmic), pointing out the Cancer Gene Census set, and predicting the effect of the mutations on protein structure and function with SNPeff (29).

Moreover, based on WES data, the analysis of amplifications and large deletions was performed making a consensus between Control FREEC (http://boevalab.com/FREEC) and ADTEX (http://adtex.sourceforge.net) with paired tumor/matched normal samples. Also, a filtering procedure was applied taking into account the uncertainty value given by Control FREEC (<80%) and the polymorphic copy-number variants from the Database of Human Genomic Variants (http://dgv.tcag.ca/dgv/app/home).

Sanger sequencing and quantitative RT-PCR

Relevant mutations were validated on tumor and PB DNA using specific primers and the Sanger sequencing method, as described previously (5). qPCR amplification of ASCL1, GAPDH, and GUSB was performed with real-time LightCycler 480 instrument (Roche). The ASCL1 mRNA expression level was evaluated on 4 *quadruple* WT GIST in comparison with 3 SDH-deficient and 5 KIT/PDGFRA-mutated GIST. Relative

expression was estimated by the DDCt method, using GAPDH and GUSB genes as housekeeping controls.

Results

Gene expression and miRNA profiling

To define the gene expression signature of *quadruple* WT GIST, we performed WTS in 4 *quadruple* WT GIST (GIST127, GIST133, GIST400, and GIST401) and compared it with the other GIST molecular subsets (2 SDH-deficient and 7 KIT-mutant and 5 PDGFRA-mutant). Unsupervised principal component analysis showed that the four subgroups cluster separately, highlighting that the *quadruple* WT GIST are a separate entity than the other molecular subgroups of GIST (Fig. 1A).

Supervised analysis resulted in 224 over and 23 underexpressed genes in quadruple WT GIST (FDR-corrected $P < 0.05$; Fig. 1B), in

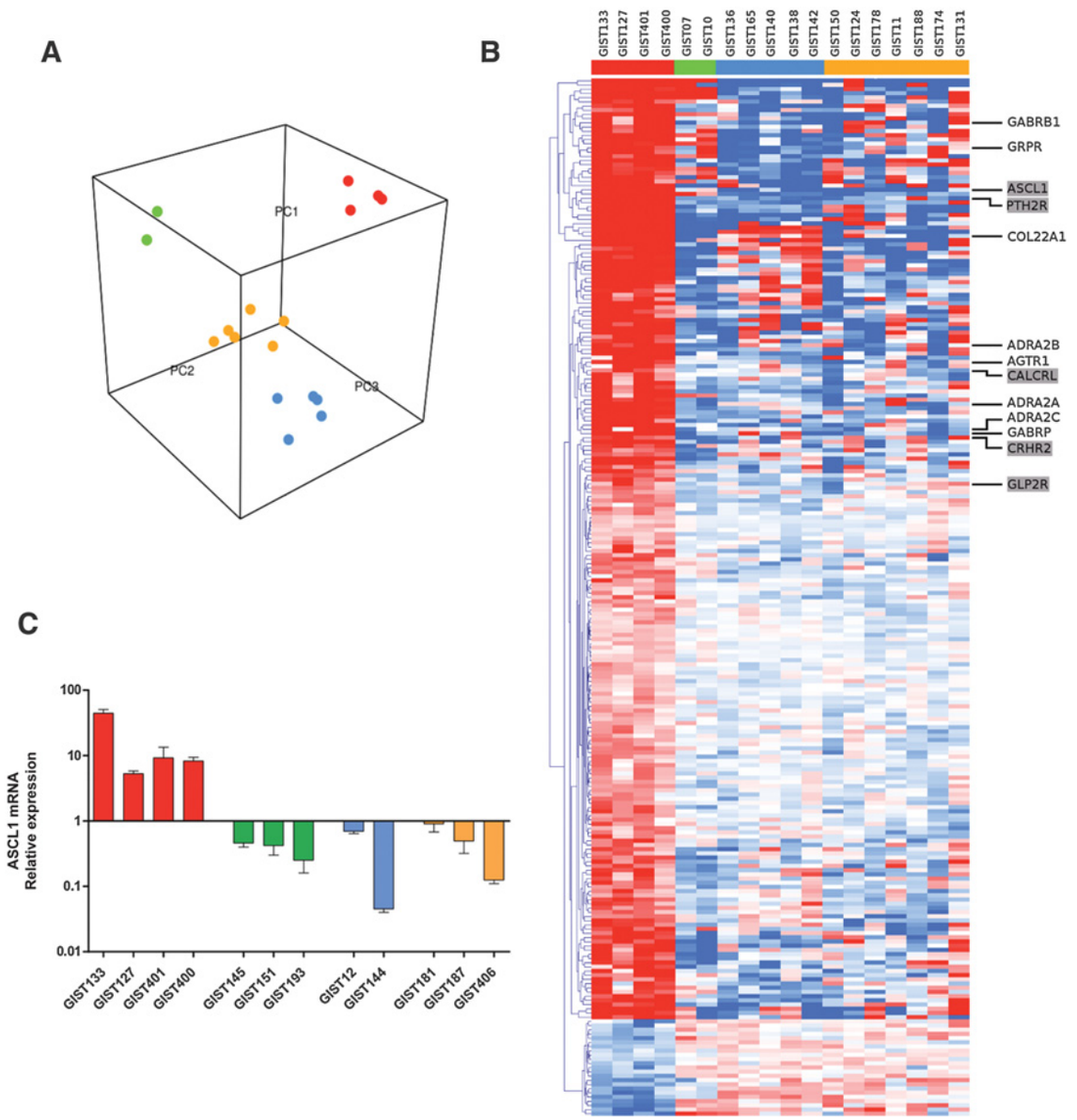

Figure 1.

Gene expression of *quadruple* WT GIST. **A,** Three-dimensional representation of principal component analysis. The *quadruple* WT GIST (red), SDH (green), PDGFRA (blue), and KIT (yellow) mutated GIST cluster separately from each other. In particular, the *quadruple* WT subgroup can be separated along the second component (PC2 axis), indicating a strong evidence of a specific gene expression profile. **B,** Heat map representing the 247 differential expressed genes (q-value < 0.05) in the comparison between *quadruple* WT and mutated GIST. Enriched genes of Neuroactive ligand–receptor interaction pathway are shown on the right of the heat map. The neuroendocrine tumor genes are highlighted in gray. **C,** qRT-PCR evaluation of the ASCL1 mRNA expression level in an additional cohort of 8 SDH or KIT/PDGFRA mutated GIST. ASCL1 relative expression was calculated in 4 quadruple WT (red), in 3 SDH-deficient (green), and in 5 KIT/PDGFRA-mutated GIST (yellow and blue, respectively).

which it was possible to confirm the expression of molecular markers characteristic of this subgroup, including the COL22A1 and CALCRL genes (22).

Functional enrichment analysis highlighted 10 significantly enriched pathways (Supplementary Table S1), many related to a neural phenotype. In particular, the *Neuroactive ligand–receptor interaction* pathway was enriched, and interestingly some of the genes involved in this pathway belong to the Secretin family (Class B) G protein–coupled receptors (PTH2R, CALCRL, CRHR2, and GLP2R) and are overexpressed in the *quadruple* WT GIST (Fig. 1B). The neural-like background was also supported by the overexpression of the transcription factor ASCL1, a commitment lineage marker of neuroendocrine tumors (30), that was the most differentially expressed (FC = 10.7) between *quadruple* WT GIST and all the other GIST classes. In an additional cohort of 8 GIST (SDH or KIT/PDGFRA mutated), it was possible to confirm that ASCL1 mRNA expression was a specific feature of only the quadruple WT subgroup (Fig. 1C).

To fully define the signature of *quadruple* WT GIST we analyzed the miRNA expression profile against KIT/PDGFRA-mutant and KIT/PDGFRA WT-SDH-deficient GIST. A total of 66 differentially expressed miRNA were identified as specific of *quadruple* WT GIST (Fig. 2A; FDR $P < 0.05$).

The integration of gene expression levels with the targets of differentially expressed miRNA allowed the identification of a network of interactions where we identified 17 miRNA as putative regulators of the genes of neuroendocrine lineage and Neuroactive ligand–receptor interaction pathway (Fig. 2B). miRNAs predicted as regulators of signature genes are reported in Supplementary Table S2.

Mutational profile

WES was performed on 9 *quadruple* WT GIST (4 fresh frozen and 5 FFPE tumor samples) and on matched normal DNA. An average of 60.5 million of reads per sample was obtained producing an average coverage per sample ranging from 54× to 76×. It is known that KIT/PDGFRA wild-type GIST can carry germline mutations in cancer-predisposing genes, including SDHA (already excluded) or NF1. Therefore, we initially analyzed whole exome data from matched normal DNA and then mapped the resulting NF1 variants on the HGMD and ClinVar databases. In this way, we identified two extremely rare germline variations: a p.R2594L in GIST268 (ExAC frequency = 2/121378) and a p.H1374Y in GIST279 (ExAC frequency = 1/118856), both recorded in ClinVar as variations of uncertain significance, and not present in the HGMD database. The NF1 germline alteration in GIST279 was previously described (24).

Copy-number analysis showed that all the *quadruple* WT tumor samples carried multiple regions of copy-number gains and losses (3–12 regions with copy-number alterations/sample), which are anyway not recurrent within the cohort. The only frequently altered genomic regions are those characteristic of KIT/PDGFRA-mutant GIST, with 6 of 9 samples showing at least one deletion in either 1p, 14q, or 22q chromosome arms (Supplementary Fig. S1 and Supplementary Table S3).

WES of tumor samples and matched normal DNA identified an average of 18 somatic mutations per sample (range, 6–29) (Supplementary Table S4). No somatic alterations in NF1 were identified in our population. The mutational profile did not show any other highly recurrent alteration shared by the majority of the cases. However, it was possible to identify a relevant oncogenic mutation in 6 of the 9 cases (Table 2 and Fig. 3).

GIST257 carried two distinct somatic mutations on TP53, leading to double inactivation of the protein, a frameshift deletion (p.S227fs*18) and a missense mutation predicted as pathogenic and recurrently mutated in multiple neoplasms (p.R158L; COSM10714).

GIST268 carried a frameshift deletion on MAX (c.100_110del; p.K34fs*31), which leads to a premature stop codon. Interestingly, this patient also carried the very rare missense germline NF1 variant (R2573L) that is recorded in the ClinVar database.

GIST320 was shown to carry a homozygous somatic frameshift deletion in the MEN1 gene (c.249_252delGTCT; p.I83fs*34), already reported in COSMIC as a recurrent event (COSM23398). This patient also showed a somatic missense mutation in TP53 (c.646G>A; p.V216M) that is frequently mutated in different tumor histotypes (74 reported cases in COSMIC: COSM10667).

GIST401 showed a somatic frameshift mutation in CHD4 (c.2659delC; p.R887fs*14), a component of the histone deacetylase NuRD complex that was recently added to the Cancer Gene Census list (http://cancer.sanger.ac.uk/census/).

GIST127 showed a complex Ins/del in the *CTNND2* gene (c.2986–2987 del/ins AG>T), which leads to loss of the reading frame and premature protein truncation. CTNND2 was shown to be a mutational hotspot in glioblastoma, linked to loss of expression (31).

This sample also carried several other genetic alterations, detected by fusion transcript analysis from WTS data and validated by Sanger sequencing (Supplementary Fig. S2). All the chimeric transcripts led to inactivation of the proteins, apart from MARK2–PPFIA1, which should cause the deregulation of PPFIA1 expression, controlled by a different promoter region. Among inactivating fusions, we detected a SPRED2-NELFCD chimera that loses all the functional domains of the two proteins, and an event of duplication and inversion of RTKN2 locus that determined the insertion of a lnRNA downstream of the exon 8 of TET1, causing the loss of TET1 reading frame and the introduction of a premature stop codon.

A FGFR1 somatic missense mutation (c.1638C>A; p.N546K) was detected in GIST409. This alteration is already reported in the COSMIC database as a hotspot mutation in CNS and soft-tissue tumors.

Discussion

The WES and gene expression analysis of *quadruple* WT GIST reveal that this subset of patients presents a homogeneous signature profile driven by an underlying molecular heterogeneity. Several mutations were also identified in the same tumors, with an average of 18 somatic mutations per sample; interestingly, despite the small samples size, no highly recurrent and shared events were found in all patients. However, excluding the germline variation of uncertain significance in NF1, in 6 out of 9 cases it was possible to identify at least one alteration in relevant potential driver genes.

In two cases we detected three pathogenic TP53 mutations, two of which in the same patient, supporting the likely role of this gene in an important fraction of *quadruple* WT GIST (>20%). As it is well known, the TP53 gene is involved in DNA repair activation and apoptosis initiation. For several decades, the role

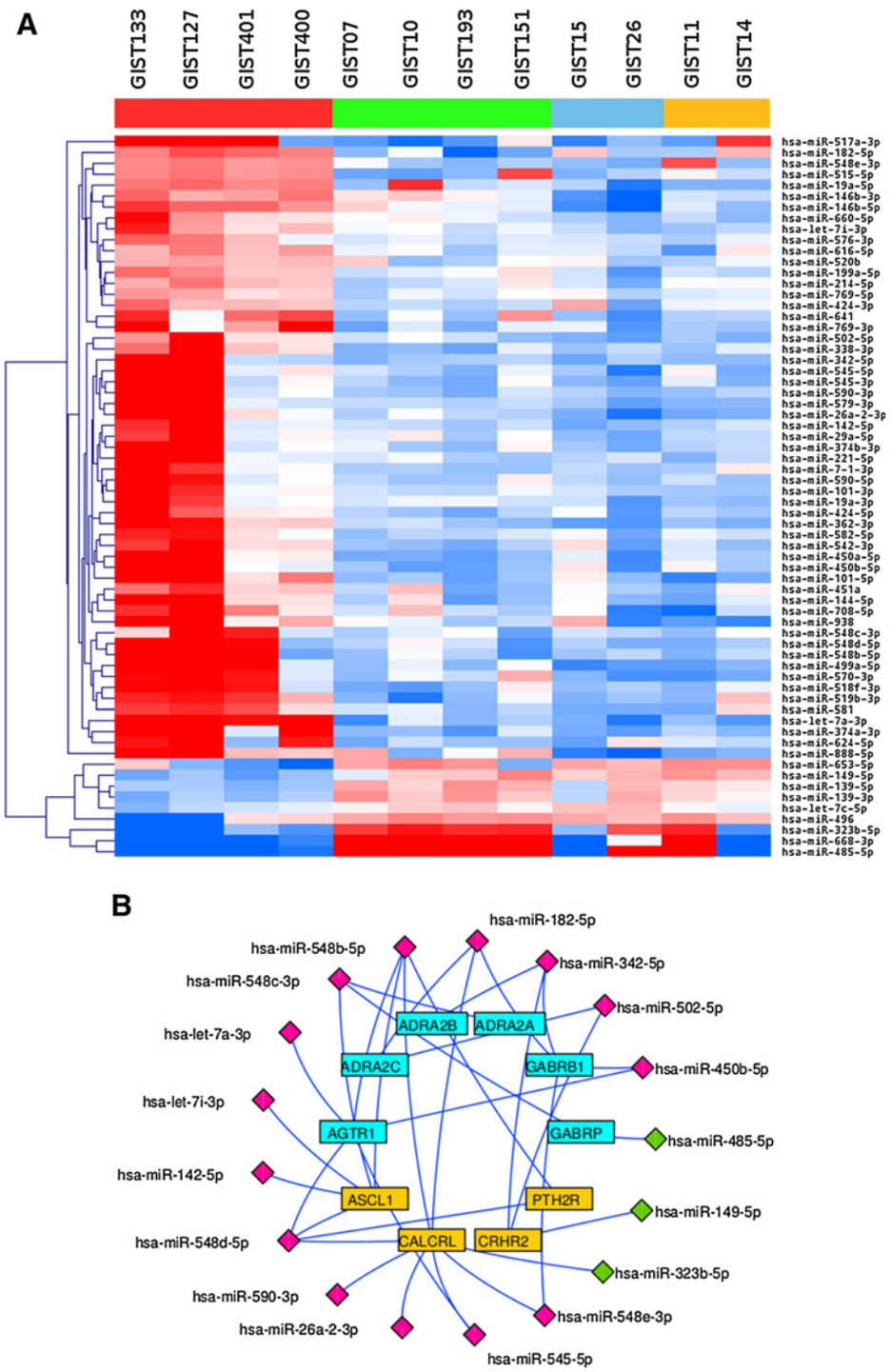

Figure 2.
miRNA expression of quadruple WT GIST. **A,** Heatmap showing the 66 differentially expressed miRNA in *quadruple* WT GIST. **B,** Correlation miRNA-mRNA: 17 miRNA were identified as putative regulators of 10 Neuroactive ligand-receptor signature genes. The neuroendocrine lineage genes were highlighted in yellow blocks. The overexpressed and underexpressed miRNA are colored in pink and green, respectively.

of TP53 deregulation in carcinogenesis has been studied in human cancers and associated with both the loss of tumor-suppressing function and the oncogenic function (32). The negative prognostic role of TP53 gene overexpression and its correlation with the increased malignant risk in GIST have been already described (33). However, to our knowledge, specific TP53 mutations have never been described in GIST patients. Therefore, the potential role in GIST development and progression of the novel mutations we identified should be further investigated.

MAX was found mutated in one case. MAX is a transcription factor and belongs to the MYC/MAX/MXD network functionally linked to cell-cycle arrest and differentiation. MAX mutation has been found very rarely involved in hereditary

Table 2. List of oncogenic mutations identified in quadruple WT GIST samples

ID	Gene	cDNA	Protein	Position	Tumor ratio	Somatic/germline
GIST127	CTNND2	c.2986_2987delinsAG>T	p.S996delinsW	chr5:11022893	0,31	Somatic
GIST257	TP53[a,b]	c.473G>T	p.R158L	chr17:7578457	0,40	Somatic
	TP53[a]	c.680delC	p.S227fs*18	chr17:7577601	0,27	Somatic
GIST268	MAX[a]	c.100_110delTCCCTACGTTT	p.K34fs*31	chr14:65560487	0,29	Somatic
	NF1[a]	c.G7781T	p.R2594L	chr17:29684020	0,41	Germline
GIST279	NF1[a]	c.C4120T	p.H1374Y	chr17:29579965	0,44	Germline
GIST320	MEN1[a,b]	c.249_252delAGAC	p.L83fs*34	chr11:64577330	0,93	Somatic
	TP53[a,b]	c.646G>A	p.V216M	chr17:7578203	0,65	Somatic
GIST401	CHD4[a]	c.2659delC	p.R887fs*14	chr12:6701977	0,47	Somatic
GIST409	FGFR1[a,b]	c.1638C>A	p.N546K	chr8:38274849	0,59	Somatic

[a]Gene included in the Cancer Gene Census list.
[b]Same mutation presents in the COSMIC database.

pheochromocytomas/paragangliomas (PCC/PGL) lacking other mutations in susceptibility genes and rarely in sporadic cases. With regard to GIST patients, a previous report firstly identified a MAX somatic truncating frameshift mutation (c.160delC; p.Gln54Lysfs*10) in a *quadruple* WT GIST and interestingly, both that case and our patient carried also additional events in NF1 (23). The previous patient carried a two-base insertion (c.6781_6782insTT; p.His2240Leufs*4) in the tumor that was not seen in the normal DNA, whereas our patient carried a missense germline NF1 rare variant. Even though this coincidence can be considered very rare and interesting at the same time, no definitive conclusions can be drawn on the association between NF1 and MAX genes in these two patients.

A homozygous MEN1 deletion was detected in one quadruple WT GIST. MEN1 is the tumor suppressor gene implicated in the Multiple endocrine neoplasia type 1 (MEN1) hereditary cancer syndrome, which is characterized by various combinations of

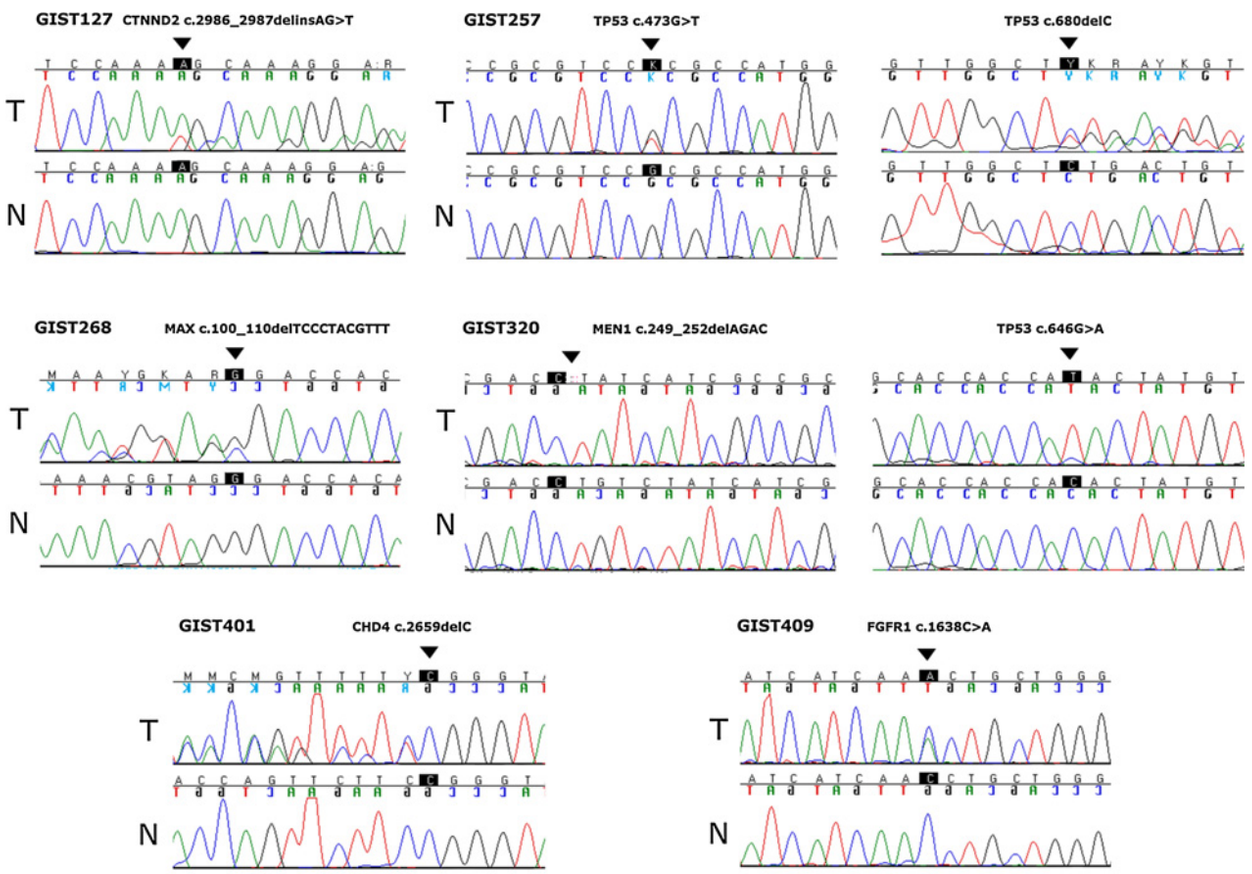

Figure 3.
Somatic mutations identified in *quadruple* WT GIST. All relevant somatic mutations were validated by Sanger sequencing and chromatograms obtained from tumor (T) and its normal counterpart (N) are shown.

endocrine neoplasia, and combinations of these tumors may be different in members of the same family (34, 35). To the best of our knowledge, the identification of MEN1 mutation in GIST is a novel finding.

The MAX and MEN1 gene mutations further extend the list of genes characterizing the neuroendocrine tumors (NET) family, along with NF1 and SDH, which are also implicated in the pathogenesis of KIT/PDGFRA wild-type GIST. NETs are a large family of diseases that generally occur as sporadic isolated tumors, sometimes also as part of complex familial endocrine cancer syndromes (35). Somatic and germline mutations of several susceptibility genes may lead to the development of NETs and many of them are shared by GIST lacking KIT/PDGFRA mutations. In fact, the current molecular knowledge underlines that among the KIT/PDGFRA WT GIST, a subgroup presents a deregulation of the SDH complex, another subgroup harbors germline and/or somatic mutations in NF1 associated or not to a clinical NF1 syndrome, and a subgroup of *quadruple* WT GIST harbors mutations in MAX and MEN1; therefore, all these subgroups can be associated with the neuroendocrine family. The four *quadruple WT* GIST studied in the present work showed a marked upregulation of ASCL1, an early immunohistochemical marker of neuroendocrine lineage, also playing a role in neural commitment, and of the genes belonging to the Class B Secretin family of G-protein–coupled receptors. In addition, a high relative expression of neural markers in a subset of SDH-intact WT GIST has been reported (36). Moreover, in the past we found that the gene expression profiles of 4 KIT/PDGFRA WT GIST—2 of them SDH deficient—profoundly differed from that of KIT/PDGFRA-mutated GIST, especially in the expression of those genes primarily restricted to neural tissues (37). Therefore, all these findings may reinforce the hypothesis that a great majority of KIT/PDGFRA WT GIST may derive from a cell at a different step of differentiation towards neural features or from a different cell of origin showing neuroendocrine commitment.

In the present study, other additional events in several genes were found. A frameshift deletion was detected in CHD4, a component of the Mi2–NuRD complex, which couples chromatin remodeling and histone deacetylation involved in transcriptional regulation, replication, DNA repair, and cell fate determination. Recently, CHD4 and several other components of the chromatin remodeling process were found recurrently mutated in several tumors (38, 39). Interestingly, MEN1 and MAX are also involved in epigenetic regulation and chromatin modifications (40, 41).

One truncating mutation in CTNND2 (δ-Catenin) was detected in one case. This gene is expressed in normal brain and is commonly overexpressed in several cancers. However, several somatic frameshift mutations are recorded in the COSMIC database, and loss-of-function mutations were identified in glioblastoma and pancreatic adenocarcinoma (31, 42). Moreover, in the same patients, several chromosomal rearrangements were detected that lead to premature stop of relevant genes, such as TET1 and SPRED2. Accumulating evidence indicates SPRED2, an inhibitor of the Ras/ERK signal transduction, as a tumor suppressor, and decreased levels of SPRED2 were associated with increased tumor invasiveness and metastasis (43). However, whether these alterations have an impact on GIST biology still needs to be assessed.

Finally, a FGFR1 somatic missense mutation was detected in one patient. FGFR1 is involved in several soft-tissue sarcoma and central nervous system tumors, and the same mutation we detected was also found in Ewing sarcoma (44). In GIST, the involvement of FGFR1 has been reported as one missense mutation and two fusion events (FGFR1–HOOK3 and FGFR1–TACC1) in quadruple WT GIST (45, 46); however, no other detailed reports on the FGFR1 deregulated pathway are already available in this disease. The FGFR1–TACC1 is the second fusion event associated with GIST along with ETV6–NTRK3 (25, 45, 46). In particular, in a recent report, these oncogenic translocations were observed in two of five cases, and the authors suggested to routinely test the translocation in *quadruple* WT GIST. However, these events were not found in our *quadruple* WT GIST patients; overall, the great difference observed regarding gene fusions between these two GIST populations confirms that the *quadruple* WT GIST can be considered a greatly heterogeneous cancer group that, in the future, could not be considered as a unique family anymore.

As a general clinical consideration, our findings do not help to profile the clinical characteristics of *quadruple* WT GIST. The only common aspect is the "non-gastric" site of the disease in a context with different gender and variable age of patients, variable disease presentation, and outcome, so a genotype–phenotype correlation cannot be hypothesized. For this reason, one challenging perspective in *quadruple* WT GIST is to enlarge the sample series as much as possible to collect more patients' data helpful to define a clinical classification and disease outcome.

In conclusion, our study showed that *quadruple* WT GIST present a homogeneous expression profile profoundly different from other GIST subsets. However, *quadruple* WT GIST show a great molecular heterogeneity, driven by different mutational events in several genes. So, the *quadruple* WT GIST that until now was a group defined as the subset of GIST that lack abnormalities of KIT, PDGFRA, SDH, and the RAS signaling pathway today can be considered as a large number of heterogeneous single entities with different molecular alterations. Among the mutational events identified in our population, the MEN1 and MAX gene involvement seems very interesting. These findings, together with the high number of tumor susceptibility genes, indicate that *quadruple* WT GIST seem to behave as neuroendocrine tumors. In fact, this picture resembles that of pheochromocytomas or other neuroendocrine tumors, characterized by a great variability in oncogenic driver genes, that ends up in a rather specific and characteristic gene expression profile. Further efforts are needed to understand if all these genomic events may represent secondary molecular hits implicated in tumor progression or the early causative event in quadruple WT GIST pathogenesis, in order to devise new targeted therapeutic strategies in this heterogeneous subset of GIST.

Disclosure of Potential Conflicts of Interest

M.A. Pantaleo has expert testimony from an entity. A. Gronchi has received speakers bureau honoraria from and is a consultant/advisory board member of Novartis, Pfizer, and Bayer. G. Grignani is a consultant/advisory board member for Novartis, Pfizer, Bayer, Lilly, and Pharmamar. P.G. Casali has received speakers bureau honoraria from Bayer, Novartis, and Pfizer, is a consultant/advisory board member for Bayer, Blueprint Medicines, Novartis, and Pfizer. No potential conflicts of interest were disclosed by the other authors.

Authors' Contributions

Conception and design: M.A. Pantaleo, M. Urbini, V. Indio, G. Ravegnini, M. Nannini, B. Vincenzi, S. Stacchiotti, A. Astolfi, G. Biasco

Development of methodology: M.A. Pantaleo, M. Urbini, V. Indio, G. Ravegnini, M. De Luca, G. Tarantino, P. Paterini, C. Ceccarelli, A. Altimari, E. Gruppioni, A. Astolfi

Acquisition of data (provided animals, acquired and managed patients, provided facilities, etc.): M.A. Pantaleo, M. Nannini, A. Gronchi, B. Vincenzi, G. Grignani, C. Colombo, E. Fumagalli, L. Gatto, M. Saponara, M. Ianni, P. Paterini, D. Santini, M.G. Pirini, S.L. Renne, P. Collini, S. Stacchiotti, G. Brandi, P.G. Casali, A.D. Pinna

Analysis and interpretation of data (e.g., statistical analysis, biostatistics, computational analysis): M.A. Pantaleo, M. Urbini, V. Indio, G. Ravegnini, M. De Luca, G. Tarantino, A. Gronchi, M. Saponara, D. Santini, S.L. Renne, P. Collini, A. Astolfi, G. Biasco

Writing, review, and/or revision of the manuscript: M.A. Pantaleo, M. Urbini, V. Indio, G. Ravegnini, M. Nannini, S. Angelini, A. Gronchi, G. Grignani, E. Fumagalli, M. Saponara, S.L. Renne, P. Collini, S. Stacchiotti, P.G. Casali, A. Astolfi

Administrative, technical, or material support (i.e., reporting or organizing data, constructing databases): M.A. Pantaleo, M. Urbini, V. Indio, G. Ravegnini, M. De Luca, G. Tarantino, S.L. Renne, P. Collini, A. Astolfi

Study supervision: M.A. Pantaleo, M. Urbini, V. Indio, M. Nannini, M. De Luca, A. Gronchi, M. Saponara, A. Astolfi

Acknowledgments

The authors extend special thanks to the GIST Study Group members, University of Bologna, Bologna, Italy: Maria Astorino, Rita Casadio, Paolo Castellucci, Fausto Catena, Massimo Del Gaudio, Monica Di Battista, Antonia D'Errico, Giorgio Ercolani, Stefano Fanti, Michelangelo Fiorentino, Cristian Lolli, Anna Mandrioli, Pier-Luigi Martelli, Nico Pagano, Paola Tomassetti, Valerio Di Scioscio, and Maurizio Zompatori

Grant Support

The present study was supported by Italian Association for Cancer Research AIRC, My First Grant 2013 and Fondazione Isabella Seragnoli, Bologna, Italy (M.A. Pantaleo).

The costs of publication of this article were defrayed in part by the payment of page charges. This article must therefore be hereby marked *advertisement* in accordance with 18 U.S.C. Section 1734 solely to indicate this fact.

Received October 29, 2016; revised December 10, 2016; accepted January 4, 2017; published OnlineFirst January 27, 2017.

References

1. Corless CL, Barnett CM, Heinrich MC. Gastrointestinal stromal tumours: origin and molecular oncology. Nat Rev Cancer 2011;11:865–78.
2. Miettinen M, Wang ZF, Sarlomo-Rikala M, Osuch C, Rutkowski P, Lasota J. Succinate dehydrogenase-deficient GISTs: a clinicopathologic, immunohistochemical, and molecular genetic study of 66 gastric GISTs with predilection to young age. Am J Surg Pathol 2011;35:1712–21.
3. Gill AJ, Chou A, Vilain R, Clarkson A, Lui M, Jin R, et al. Immunohistochemistry for SDHB divides gastrointestinal stromal tumors (GISTs) into 2 distinct types. Am J Surg Pathol 2010;34:636–44.
4. Janeway KA, Kim SY, Lodish M, Nosé V, Rustin P, Gaal J, et al. Defects in succinate dehydrogenase in gastrointestinal stromal tumors lacking KIT and PDGFRA mutations. Proc Natl Acad Sci U S A 2011;108:314–8.
5. Pantaleo MA, Astolfi A, Urbini M, Nannini M, Paterini P, Indio V, et al. Analysis of all subunits, SDHA, SDHB, SDHC, SDHD, of the succinate dehydrogenase complex in KIT/PDGFRA wild-type GIST. Eur J Hum Genet 2014;22:32–9.
6. Pantaleo MA, Astolfi A, Indio V, Moore R, Thiessen N, Heinrich MC, et al. SDHA loss-of-function mutations in KIT-PDGFRA wild-type gastrointestinal stromal tumors identified by massively parallel sequencing. J Natl Cancer Inst 2011;103:983–7.
7. Miettinen M, Killian JK, Wang ZF, Lasota J, Lau C, Jones L, et al. Immunohistochemical loss of succinate dehydrogenase subunit A (SDHA) in gastrointestinal stromal tumors (GISTs) signals SDHA germline mutation. Am J Surg Pathol 2013;37:234–40.
8. Killian JK, Kim SY, Miettinen M, Smith C, Merino M, Tsokos M, et al. Succinate dehydrogenase mutation underlies global epigenomic divergence in gastrointestinal stromal tumor. Cancer Discov 2013;6:648–57.
9. Mason EF, Hornick JL. Succinate dehydrogenase deficiency is associated with decreased 5-hydroxymethylcytosine production in gastrointestinal stromal tumors: implications for mechanisms of tumorigenesis. Mod Pathol 2013;26:1492–7.
10. Killian JK, Miettinen M, Walker RL, Wang Y, Zhu YJ, Waterfall JJ, et al. Recurrent epimutation of SDHC in gastrointestinal stromal tumors. Sci Transl Med 2014;6:268ra177.
11. Urbini M, Astolfi A, Indio V, Heinrich MC, Corless CL, Nannini M, et al. SDHC methylation in gastrointestinal stromal tumors (GIST): a case report. BMC Med Genet 2015;28;16:87.
12. Kelly L, Bryan K, Kim SY, Janeway KA, Killian JK, Schildhaus HU, et al. Post-transcriptional dysregulation by miRNAs is implicated in the pathogenesis of gastrointestinal stromal tumor [GIST]. PLoS One 2013; 8:e64102.
13. Pantaleo MA, Lolli C, Nannini M, Astolfi A, Indio V, Saponara M, et al. Good survival outcome of metastatic SDH-deficient gastrointestinal stromal tumors harboring SDHA mutations. Genet Med 2015;17:391–5.
14. Nannini M, Astolfi A, Paterini P, Urbini M, Santini D, Catena F, et al. Expression of IGF-1 receptor in KIT/PDGF receptor-α wild-type gastrointestinal stromal tumors with succinate dehydrogenase complex dysfunction. Future Oncol 2013;9:121–6.
15. Belinsky MG, Rink L, Flieder DB, Jahromi MS, Schiffman JD, Godwin AK, et al. Overexpression of insulin-like growth factor 1 receptor and frequent mutational inactivation of SDHA in wild-type SDHB-negative gastrointestinal stromal tumors. Genes Chromosomes Cancer 2013;52: 214–24.
16. Pasini B, McWhinney SR, Bei T, Matyakhina L, Stergiopoulos S, Muchow M, et al. Clinical and molecular genetics of patients with the Carney-Stratakis syndrome and germline mutations of the genes coding for the succinate dehydrogenase subunits SDHB, SDHC, and SDHD. Eur J Hum Genet 2008;16:79–88.
17. Zhang L, Smyrk TC, Young WF Jr, Stratakis CA, Carney JA. Gastric stromal tumors in Carney triad are different clinically, pathologically, and behaviourally from sporadic gastric gastrointestinal stromal tumors: findings in 104 cases. Am J Surg Pathol 2010;34:53–64.
18. Haller F, Moskalev EA, Faucz FR, Barthelmeß S, Wiemann S, Bieg M, et al. Aberrant DNA hypermethylation of SDHC: a novel mechanism of tumor development in Carney triad. Endocr Relat Cancer 2014; 21:567–77.
19. Daniels M, Lurkin I, Pauli R, Erbstösser E, Hildebrandt U, Hellwig K, et al. Spectrum of KIT/PDGFRA/BRAF mutations and phosphatidylinositol-3-kinase pathway gene alterations in gastrointestinal stromal tumors (GIST). Cancer Lett 2011;312:43–54.
20. Bajor J. Gastrointestinal stromal tumors in patients with type 1 neurofibromatosis. Clin Exp Med J 2009;3:247–54.
21. Pantaleo MA, Nannini M, Corless CL, Heinrich MC. Quadruple wild-type (WT) GIST: defining the subset of GISTs that lack abnormalities of KIT, PDGFRA, SDH, and the RAS signalling pathway. Cancer Med 2015;4:101–3.
22. Nannini M, Astolfi A, Urbini M, Indio V, Santini D, Heinrich MC, et al. Integrated genomic study of quadruple-WT GIST (KIT/PDGFRA/SDH/RAS pathway wild-type GIST). BMC Cancer 2014;14:685.
23. Belinsky MG, Rink L, Cai KQ, Capuzzi SJ, Hoang Y, Chien J, et al. Somatic loss of function mutations in neurofibromin 1 and MYC associated factor X genes identified by exome-wide sequencing in a wild-type GIST case. BMC Cancer 2015;15:887.
24. Gasparotto D, Rossi S, Polano M, Tamborini E, Lorenzetto E, Sbaraglia M, et al. Quadruple-negative GIST is a sentinel for unrecognized Neurofibromatosis Type 1 syndrome. Clin Cancer Res 2016; Jul 7. pii: clincanres. 0152.2016.
25. Brenca M, Rossi S, Polano M, Gasparotto D, Zanatta L, Racanelli D, et al. Transcriptome sequencing identifies ETV6-NTRK3 as a gene fusion involved in GIST. J Pathol 2015;238:543–9.
26. Boikos SA, Pappo AS, Killian JK, LaQuaglia MP, Weldon CB, George S, et al. Molecular subtypes of KIT/PDGFRA wild-type gastrointestinal stromal

tumors: a report from the National Institutes of Health Gastrointestinal Stromal Tumor Clinic. JAMA Oncol 2016;2:922–8.
27. Kim D, Pertea G, Trapnell C, Pimentel H, Kelley R, Salzberg SL. TopHat2: accurate alignment of transcriptomes in the presence of insertions, deletions and gene fusions. Genome Biol 2013;14:R36.
28. Li H, Durbin R. Fast and accurate short read alignment with Burrows-Wheeler transform. Bioinformatics 2009;25:1754–60.
29. Cingolani P, Platts A, Wang le L, Coon M, Nguyen T, Wang L, et al. A program for annotating and predicting the effects of single nucleotide polymorphisms, SnpEff: SNPs in the genome of Drosophila melanogaster strain w1118; iso-2; iso-3. Fly (Austin). 2012;6:80–92.
30. Chen H, Biel MA, Borges MW, Thiagalingam A, Nelkin BD, Baylin SB, et al. Tissue-specific expression of human achaete-scute homologue-1 in neuroendocrine tumors: transcriptional regulation by dual inhibitory regions. Cell Growth Differ 1997;8:677–86.
31. Frattini V, Trifonov V, Chan JM, Castano A, Lia M, Abate F, et al. The integrated landscape of driver genomic alterations in glioblastoma. Nat Genet 2013;45:1141–9.
32. Muller PA, Vousden KH. P53 mutations in cancer. Nat Cell Biol 2013;15:2–8.
33. Zong L, Chen P, Xu Y. Correlation between P53 expression and malignant risk of gastrointestinal stromal tumors: evidence from 9 studies. Eur J Surg Oncol 2012;38:189–95.
34. Giusti F, Marini F, Brandi ML. Multiple Endocrine Neoplasia Type 1. 2005 Aug 31 [updated 2015 Feb 12]. In: Pagon RA, Adam MP, Ardinger HH, Wallace SE, Amemiya A, Bean LJH, Bird TD, Fong CT, Mefford HC, Smith RJH, Stephens K, editors. GeneReviews [Internet]. Seattle (WA): University of Washington, Seattle; 1993–2016.
35. Minetti M, Grossman A. Somatic and germline mutations in NETs: Implications for their diagnosis and management. Best Pract Res Clin Endocrinol Metab 2016;30:115–27.
36. Beadling C, Patterson J, Justusson E, Nelson D, Pantaleo MA, Hornick JL, et al. Gene expression of the IGF pathway family distinguishes subsets of gastrointestinal stromal tumors wild type for KIT and PDGFRA. Cancer Med 2013;2:21–31.
37. Pantaleo MA, Astolfi A, Nannini M, Ceccarelli C, Formica S, Santini D, et al. Differential expression of neural markers in KIT and PDGFRA wild-type gastrointestinal stromal tumours. Histopathology 2011;59:1071–80.
38. Kim MS, Chung NG, Kang MR, Yoo NJ, Lee SH. Genetic and expressional alterations of CHD genes in gastric and colorectal cancers. Histopathology 2011;58:660–8.
39. Gonzalez-Perez A, Jene-Sanz A, Lopez-Bigas N. The mutational landscape of chromatin regulatory factors across 4,623 tumor samples. Genome Biol 2013;14:r106
40. Yang YJ, Song TY, Park J, Lee J, Lim J, Jang H, et al. Menin mediates epigenetic regulation via histone H3 lysine 9 methylation. Cell Death Dis 2013;4:e583.
41. Bouchard C, Dittrich O, Kiermaier A, Dohmann K, Menkel A, Eilers M, et al. Regulation of cyclin D2 gene expression by the Myc/Max/Mad network: Myc-dependent TRRAP recruitment and histone acetylation at the cyclin D2 promoter. Genes Dev 2001;15:2042–7.
42. Nopparat J, Zhang J, Lu JP, Chen YH, Zheng D, Neufer PD, et al. δ-Catenin, a Wnt/β-catenin modulator, reveals inducible mutagenesis promoting cancer cell survival adaptation and metabolic reprogramming. Oncogene 2015;34:1542–52.
43. Yoshida T, Hisamoto T, Akiba J, Koga H, Nakamura K, Tokunaga Y, et al. Spreds, inhibitors of the Ras/ERK signal transduction, are dysregulated in human hepatocellular carcinoma and linked to the malignant phenotype of tumors. Oncogene 2006;25:6056–66.
44. Agelopoulos K, Richter GH, Schmidt E, Dirksen U, von Heyking K, Moser B, et al. Deep sequencing in conjunction with expression and functional analyses reveals activation of FGFR1 in Ewing Sarcoma. Clin Cancer Res 2015;21:4935–46.
45. Shi E, Wang K, Ross JR, Tang C-M, Harismendy O, Ali S, et al. Comprehensive genomic profiling of quadruple (KIT/PDGFRA/SDH/RAS pathway) wild-type gastrointestinal stromal tumors. CTOS 2015. Paper 030.
46. Heinrich MC, Kang G, Warrick A, Corless CL, Beadling C. Oncogenic receptor tyrosine kinase (RTK) translocations in a subset of quadruple wild-type gastrointestinal stromal tumors (GIST). J Clin Oncol 34, 2016 (suppl; abstr 11012).